



Improvements to airborne laser scanning data filtering in sandstone landscapes

M. Tomková^{a,*}, M. Potůčková^a, J. Lysák^a, M. Jančovič^a, L. Holman^a, V. Vilímek^b

^a Charles University, Faculty of Science, Department of Applied Geoinformatics and Cartography, Albertov 6, Praha 2, Czechia

^b Charles University, Faculty of Science, Department of Physical Geography and Geoecology, Albertov 6, Praha 2, Czechia

ARTICLE INFO

Keywords:

Sandstone landscape
Digital terrain model
Topographical mapping
Laser scanning
Point cloud filtering

ABSTRACT

Sandstone rock outcrops form a unique part of the landscape of Central Europe. Due to climate conditions, they are mostly covered by dense vegetation. With some limitations, laser scanning technology allows the ground to be captured even under the tree canopy, making it a powerful tool for mapping vegetated and inaccessible terrain. A challenge in deriving a digital terrain model from an acquired point cloud lies in filtering, i.e., discrimination between ground and non-ground points. Conventional filtering methods applied on complex high-energy terrain with formations resembling man-made objects, e.g., rock walls, do not provide satisfactory results with respect to the accuracy of point assignment to ground and non-ground classes and consequently terrain modelling. However, the quality of digital terrain models is critical for geomorphometric applications and recognition of spatial patterns. This study proposes three filtering methods adapted to various morphological conditions of sandstone landscape regions i.e., spatially conditioned filtering, object-oriented classification, and filtering with additional terrain data. Spatially conditioned filtering is based on a well-known method of triangulated irregular network densification, but it adjusts selected parameters in an iterative way. This has been proven to be successful in filtering sandstone rocks by the application of distinct sets of parameters to areas with and without rock formations. Object-oriented classification distinguishes between rock pillars and trees in rock cities based on features describing the distribution of points inside these objects. The method achieved an overall accuracy of 85 % with respect to manually filtered data and outperformed the conventional methods. Filtering with additional terrain data requires already filtered and co-registered references for spatial querying. Evaluation by GNSS measurements showed that the digital terrain model derived using this method achieved a higher accuracy than that derived by conventional methods.

1. Introduction

Digital terrain models belong among important data sources in geomorphological research. They are expected to be geometrically accurate, complete and up-to-date. Surveying by means of terrestrial methods (total stations, terrestrial laser scanning) are the most precise but time-consuming and not suitable for larger areas and high-energy terrains. Tree canopy prevents terrain data capturing in vegetated areas by photogrammetric methods. Airborne laser scanning (ALS) overcomes this limitation to high extent and has been widely applied in geosciences in the last two decades (e.g., Alho et al., 2011; Hayakawa and Oguchi, 2016). A large variety of geomorphological processes may be quantified, and landforms detected using ALS. Bollmann et al. (2011) utilised ALS for glacier boundary detection, deriving of mass balance,

excretion of crevasse zones, and classification of glacier surface features in a high alpine landscape. Neotectonic activity was investigated with ALS in the Little Hungarian Plain (Pannonian Basin) by Székely et al. (2009). Another example is the application of ALS in fluvial (river) geomorphology, where ALS data sets provide information on water-land-boundaries or the elevation of the riparian foreland and their roughness (Vetter et al., 2011). High resolution topography and other techniques for proper displacement identification are valuable tools for reliable description of unstable slopes (Castagnetti et al., 2014). The importance of ALS data for geomorphometric analyses of sandstone landscapes under forest, similar to study areas in the presented paper, is discussed in Jancewicz and Porębna (2022).

The sandstone phenomenon creates an unusual part of the Central European landscape. The Bohemian Cretaceous Basin, one of the most

* Corresponding author.

E-mail address: michaela.tomkova@natur.cuni.cz (M. Tomková).

<https://doi.org/10.1016/j.geomorph.2022.108377>

Received 15 December 2021; Received in revised form 16 July 2022; Accepted 16 July 2022

Available online 25 July 2022

0169-555X/© 2022 Elsevier B.V. All rights reserved.

extensive areas of sandstone in Europe, occupies the northern part of Czechia, and partially extends to Germany and Poland. Steep walls, labyrinths of deep and narrow gorges with debris at their bottoms, bizarre-shaped rocky pillars and pinnacles, and flat sandstone plateaus split by rectangular joint systems characterise probably the most fascinating localities, which in some languages are known as *rock cities* (e.g., *Felsenstadt* in German) (Migoń et al., 2017). However, the sandstone relief is not limited to rock cities, it includes assemblages of rock outcrops from small rocks hidden in forests, through larger blocks, to imposing vertical or even overhanging rock walls. Under the climate conditions of Central Europe, most sandstone areas are covered by dense vegetation, often coniferous (Härtel et al., 2007).

Surveying and mapping rugged, wooded, and often inaccessible sandstone landscapes has always been a challenging task for topographers and cartographers, and a lack of high-quality maps has made any further research in these areas complicated. Photogrammetry, as the most commonly used technique for topographic mapping, is of limited use in rugged and forested rock terrains. Aerial images usually only show rocks taller than the tree canopy, whereas large areas covered with vegetation or occluded by higher rock formations remain hidden. With ALS, a change for the better has come about. ALS provides digital 3D data with a high density (tens of points per sq. m may be easily achieved, Qin et al., 2016), and accuracy (at the level of 0.15 m standard deviation in the 3D position, Xie et al., 2020). The key feature of this technology for mapping wooded terrains is the ability of the laser pulses to penetrate the vegetation (depending on the density) whereby enabling ground points under the canopy to be measured. Although it also suffers from some disadvantages in extremely rugged terrain (e.g., areas without measurements due to the shadow of high objects), it may greatly improve the quality of information about the terrain.

The most significant drawback of ALS data in sandstone areas is hidden in the processing part. An essential task is filtering, i.e., the classification of acquired data into ground and non-ground points (Brise, 2010). The ability to filter points in the point cloud to ground points only enables a visualisation and analysis of rock outcrops. However, conventional filtering techniques do not provide satisfactory results mainly due to extreme height differences within small areas and, therefore, outcropping rock formations are deformed. Moreover, the landscape forms vary widely in sandstone areas so a single approach cannot be applied universally in all regions.

Despite the imperfections in DTMs, ALS data has been widely employed for geomorphometric applications in sandstone landscapes, including recognition of spatial patterns of canyons and joint systems, valley networks, intensive river erosion, mass movements and escarpment retreat, occurrence and distribution of boulders hidden in the forest canopy, quantification of proportions of convex and concave features, and many more. For example, Duszyński et al. (2018) investigated the evolution of boulder-filled canyons using a morphometric protection index calculated from DTM enhanced by fieldwork due to the insufficient point density for capturing the geomorphological details of the canyon network. Different trajectories in evolutionary stages of tableland determined by lithological and structural characteristics are presented in Migoń et al. (2020). Several errors in the used DTM were encountered in the study, which were solved by manual intervention in the classified point cloud. Hydrological and geomorphometric approaches were merged in the analysis of the topographic wetness index aimed at the recognition of structural connectivity in Jancewicz et al. (2019). Multiple topographic metrics and indices were used for exploration and classification of evolutionary histories of escarpments in the Stołowe Mountains tableland in Migoń and Kasprzak (2016). Jancewicz et al. (2020) presented the possibilities of using multiple national DTMs with different characteristics for geomorphometric purposes. Most of the studies concur that the results of analyses suffer from the quality of available DTMs. Some DTM properties, such as point density and occluded areas, may only be improved by more suitable data acquisition but others, such as missing rock formations and artefacts caused by

unfiltered echoes from vegetation, may be enhanced with a better performing filtering method or by manual editing. Success rate of the effort to improve DTM largely depends on the point density of the original point cloud (Jancewicz and Poręba, 2022).

The aim of this paper is to present improved ALS filtering methods leading to the higher accuracy of a derived DTM in different, but in the Central European context typical, types of sandstone landscapes. Three different solutions partially based on conventional filtering methods are proposed and experimentally tested. Iterative spatially conditioned filtering is suited to sandstone landscapes with dominating compact rock walls and plateaus. For areas characterised by rock pillars and trees in rock cities, a novel method of object-oriented filtering has been developed. Finally, a method that is dependent on existing pre-filtered (in our case, less dense) terrain data, and that is scalable to almost any type of terrain has been designed. This approach was motivated by new projects collecting ALS datasets over the same area with higher point density to update and improve existing DTMs.

2. Specifics of ALS data in high-energy vegetated terrain

Nowadays, ALS is a widely used technology with the advantages in sensing mostly independent of weather, fast acquisition of points with 3D coordinates on large areas in comparison to terrestrial methods, partial penetration of signal through tree canopy, and much more (see Shan and Toth, 2018; Vosselman and Maas, 2010). The section focuses on ALS data collected in high-energy vegetated terrain or, specifically, in sandstone landscapes from three perspectives. Firstly, aspects of data acquisition are discussed to introduce potential drawbacks that influence further work with the data. The second, most comprehensive, part describes alternative approaches to filtering ALS data for which commonly used methods do not produce satisfactory results. Finally, available datasets from sandstone landscapes in Czechia are listed with a brief description of their acquisition and processing.

2.1. Data acquisition

Some limitations arise from the rugged terrain itself. Occluded areas (i.e., areas without data; Fig. 1A) are often present due to considerable height differences and scanning geometry, and they occur more frequently when wider scanning angles (over $\pm 15^\circ$ off nadir) are used. The effect is clearly observable behind protruding rock towers or at the bottom of deep and narrow gorges. Therefore, the resulting point cloud has a highly variable point density (Fig. 1B) that complicates further processing. The occluded areas may be partially eliminated by repeated scanning using different flight directions; however, this approach extends the flight time, and subsequently the scanning and processing costs.

Other issues are related to geometric adjustment of overlapping point clouds (strips) collected from the individual flight lines of the aircraft. The complexity of a rugged sandstone terrain has a significant effect on the process of finding matching primitives in overlapping point clouds. The success of this process strongly depends on the density of the point cloud. With a density of tens of points per sq. m, objects suitable enough for cloud matching may be found on rock surfaces. If the density is lower, the point cloud is not able to fully describe the rock surface, which makes the correspondence problem an ill-posed one (Shan and Toth, 2018). With an increasing point density, smaller discrepancies after strip adjustment have a substantial negative influence on the resulting data. As the rocky features are often sharply delineated, the difference between adjusted point clouds is evident on rock faces and edges, which additionally complicates further processing, especially filtering and classification.

Dense vegetation may totally prevent echoes reaching the ground. Scanning during leaf-off periods may be a solution, but it does not help much in the case of coniferous vegetation. Generally, parts of the relief visible from above or covered by just a few branches are more

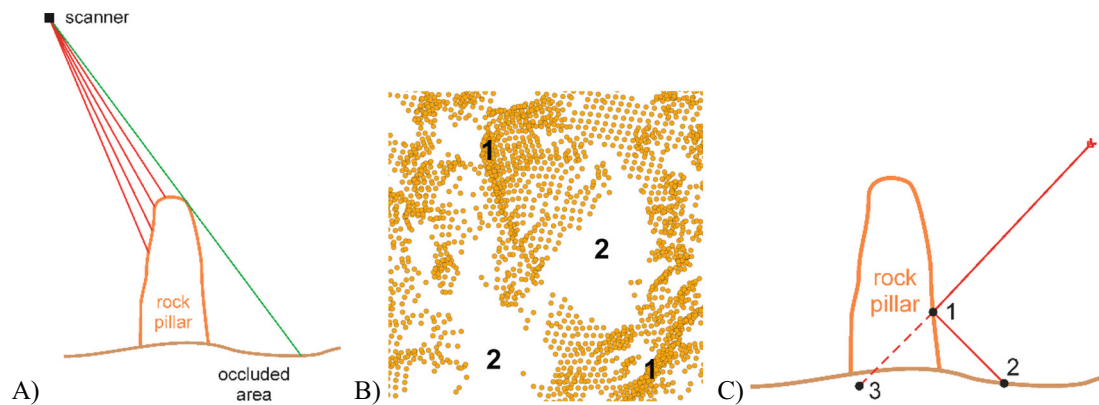


Fig. 1. Effects of rugged terrain on an ALS point cloud. A) Occluded areas due to a high rock pillar and scanning geometry. B) Visualisation of the point cloud from one flight strip - high point density on the exposed side of rock formations (1) and occluded areas (2). C) The double-bounce effect – the laser pulse firstly reaches the ground (1) and bounces (2). Coordinates of the resulting point in the point cloud (3) are calculated based on the time-of-flight and the scanning angle, and are, therefore, not correct.

thoroughly captured than hidden parts from the bottom of ravines. However, for topographic mapping it seems to be just as, or even more, important to gain information about the base of rocks, as it may form the only passable way through a rocky area without the need of climbing. In addition to lower density in clefts, the accuracy of measurements may also be affected by the multipath effect (Fig. 1C).

Due to the wide scanning angles, overhangs that may be commonly found in sandstone landscapes are frequently captured. If the output is not a 3D model of the rocks, overhangs are not desirable. Keeping the form of the bottom or the overhanging part of the rock in the DTM may cause a considerable deformation of the rock shape or cover a possible path under the overhang.

2.2. Data processing

Processing of acquired point clouds usually includes data filtering (eliminating non-ground points) or classification (discriminating echoes reflected from the ground, vegetation, building, etc.). A broad variety of filtering algorithms have been developed so far (Shan and Toth, 2018). The concept behind these algorithms is to eliminate non-ground points using a specific geometry criterion, e.g., maximum height difference for a given distance (Vosselman, 2000), maximum angle from neighbouring points (Axelsson, 2000), relative height above surface computed in a previous iteration (Kraus and Pfeifer, 1998). All these procedures usually work successfully, using a threshold dependent on the type of processed area. If a threshold is set too strictly, the resulting relief interpolated from the DTM seems to be smoother, eliminating small terrain features and causing type I errors (classification of ground points as non-ground). On the other hand, parameters that are set too loosely not only keep the microtopography of the relief, but also mark echoes reflected from low vegetation as ground points, leading to type II errors (classification of non-ground points as ground). Having a priori knowledge of relief type, it is usually possible to find a suitable threshold.

However, this approach may not succeed in a wooded and extremely rugged landscape. The assumption that points lying too high from the expected ground are non-ground points is simply not met in the case of nearly vertical walls and rock pillars. In an urban landscape, algorithms for filtering are expected to filter out both vegetation and buildings (Shan and Toth, 2018) but in rock cities, building-like structures form a part of the terrain and only vegetation needs to be filtered out. The theory has been proven multiple times in studies comparing the performance of filtering methods. For example, Sithole and Vosselman (2004) compared traditional filtering methods in various terrains and land cover types. In the case of steep slopes, errors for most of the methods increased. Similar results were observed by Zhao et al. (2018)

in vegetated mountain areas. Slopes in their test locations reached up to 40° , which can be considered as steep slopes but the rock faces in sandstone landscapes exceed this value significantly. Depending on the parameters of an employed method, sharp edges of rock plateaus are often smoothed, whole pillars are filtered out, and new terrain features are created by relics of vegetation echoes in the filtered relief of rock areas (Fig. 2).

In general, the following strategies for more successful ground point extraction in high-energy vegetated relief may be applied:

- 1) **Semi-automatic filtering.** This process combines conventional processing, i.e., filtering algorithms like TIN densification (Axelsson, 2000) or robust interpolation (Kraus and Pfeifer, 1998) followed by a manual refinement of the results. The point density is the essential parameter, especially in very rugged terrain, as without adequate sampling smaller rock features are indistinguishable from echoes coming from vegetation (Fig. 3). Two main approaches may be used, i.e., setting strict filtering parameters and manually returning the rock formations back to the ground class or setting loose parameters and then eliminating vegetation from the ground. Based on the authors' experience, the second approach seems to be more suitable if focus is on keeping as many small terrain features as possible. 2D and 3D views of point clouds may be used during manual processing. In the case of 2D views, an axonometric or profile look is often applied, with the option of interactive selection of more points. For better perceiving objects in the scene, a slight rotation in the space is very helpful, because it allows the relative 3D position of points to be understood even in 2D. The scanning pattern, depending on the scanning device used, also affects the visual interpretation to a great extent. More uniformly spaced points along lines are better for visual interpretation than irregularly intersecting wavy patterns (Fig. 4). Additional supporting information from a topographic map, database, or orthophoto may be helpful. In general, it is a very time-consuming procedure requiring both practice and good knowledge of relief characteristics. For example, this strategy was applied in Migoń et al. (2020) and for a limited scope in the Czech nationwide product DMR 5G (Dušánek, 2014, see Subsection 2.3 for more details). Jancewicz and Porębna (2022) established a semi-automatic filtering process of relatively dense point cloud (10 points per sq. m) with an automatic pre-filtering based on elevation difference threshold value (Meng et al., 2010) applied on the raster of minimum heights within the cells.
- 2) **Filtering with additional information.** Since conventional filtering methods are mostly based on the evaluation of geometric

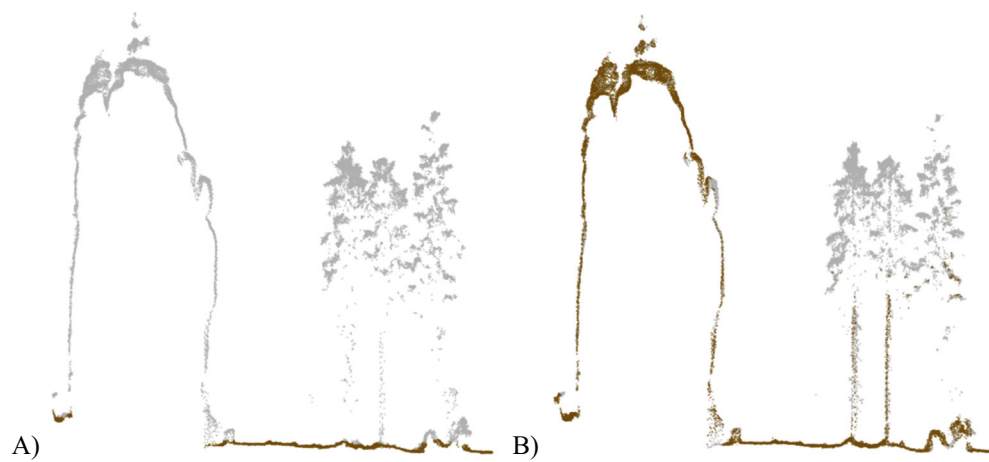


Fig. 2. Illustration of effect of setting method parameters. Profiles show results of *lasground* function from LAStools (Isenburg, 2020) applied on a very dense point cloud (hundreds of points per sq. m). Dark brown dots represent ground points and grey dots non-ground points, Strict parameters (step 5, offset 0.5) result in filtered-out rock pillar and some smaller rock features or boulders but also in precise classification of vegetation to non-ground points (A). On the contrary, loose parameters (step 0.5, offset 20) leave most of the points of the rock pillar and boulders in ground but also include tree trunks and part of the tree crown (B). (For interpretation of the references to colour in this figure legend, the reader is referred to the web version of this article.)

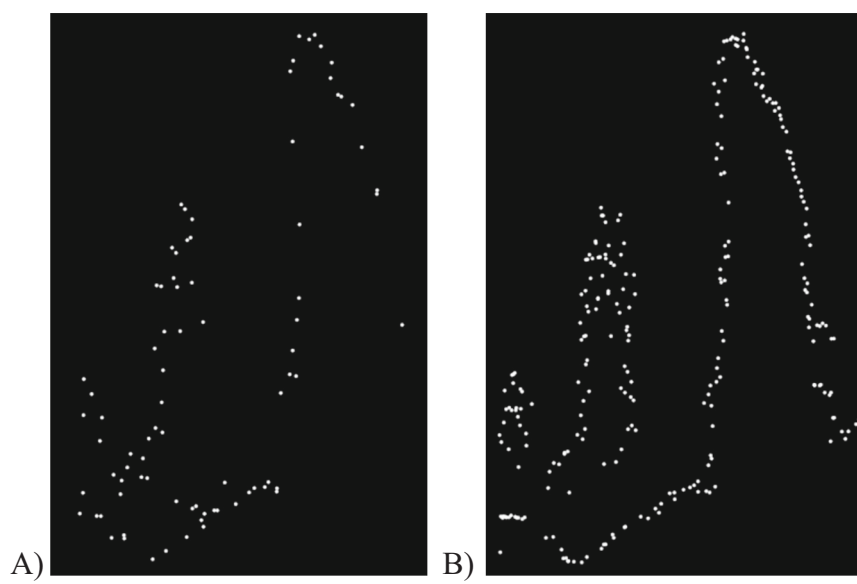


Fig. 3. Profiles of point clouds with different point densities. Density of approximately 1.5 points per sq. m (A) may not be sufficient to reliably distinguish trees and rock features. A three-time denser point cloud (B) gives a better representation of the objects (tree on the left, pillar on the right).

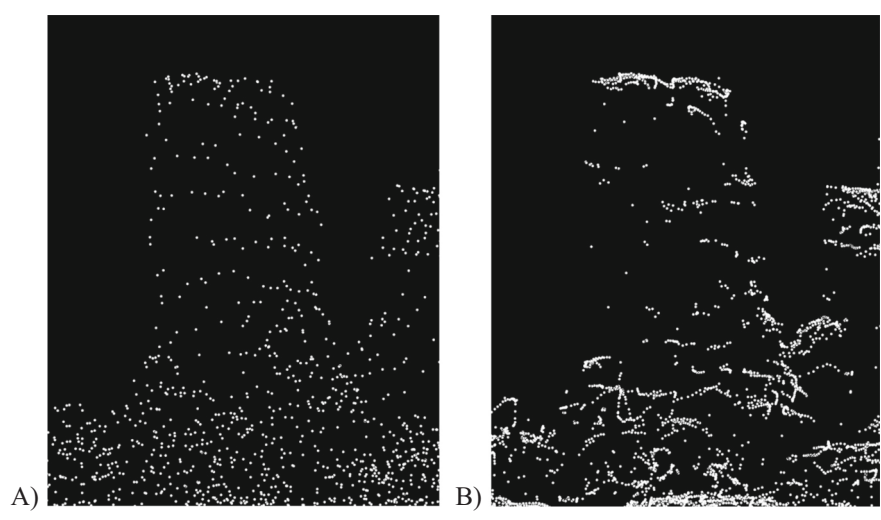


Fig. 4. Profiles of point clouds with different scanning patterns. The objects may be more easily interpreted in a point cloud with uniformly distributed points along scanning lines (A) in comparison to the wavy pattern (B) even though the number of points is more than five times smaller.

information of points, additional information may help to distinguish between ground and non-ground points. Such information may be either another property of the pulse (e.g., echo amplitude) or data from optical sensors.

- **Properties of the pulse itself.** Contemporary scanning systems support the retrieval of more information about the returned pulse than its 3D coordinates. This information, often referred to as full-waveform information, most commonly includes the order of return, total number of returns for reflected pulse, returned echo amplitude, and width (Wagner et al., 2006, 2004). Utilisation of this additional information for point cloud filtering is useful even for advanced modelling tasks. From real examples, the computation of the height difference between the first and last returns may be mentioned (Csaplovics, 2007). Another approach was presented by Doneus and Briese (2006), who used echo width to eliminate the remaining low vegetation after the filtering procedure. A more sophisticated approach of using robust interpolation to introduce this additional information as a priori weight for the individual points into filtering was presented by Mandlbürger et al. (2007). This was further elaborated by Mücke et al. (2008), who proposed considering an amplitude-dependent adaptation of the previously mentioned a priori weights, because the values of the echo width of the last points with low echo amplitude are significantly noisier. Paleček and Kubíček (2018) calculated the ratio between echo width and amplitude to filter data in rocky landscapes. Based on the results of the studies mentioned above, the role of additional pulse information for data filtering seems to be more supplementary than crucial.
 - **Information from an optical sensor.** Information from an optical sensor (red, green, blue and/or infrared bands), preferably taken simultaneously with a laser scanning campaign, may also be considered. Extreme care must be taken while orthorectifying the aerial images, as even a small shift can devalue the usability of the attributes. Bare sandstone rocks, taller than the canopy, may be identified automatically by image classification algorithms. This approach was used in experiments with data from the GeNeSiS project (Geoinformation Networks for the cross border National Park Region of Saxon-Bohemian Switzerland – see Subsection 2.3 for details) as described in Gašior (2006). As the tops of sandstone rocks are usually very vertically broken with a network of cracks, shadows can mislead the classification, so the refinement of its result should be considered, especially for a dense point cloud. This approach is not applicable for the classification of points lying under vegetation.
- 3) **Filtering adjusted to specific terrain.** In cases where the aim is to filter just a location with specific terrain, adjusted methods may be employed. These methods often cannot compete with conventional methods when applied on different situations than they are designed for, but they outperform conventional methods if applied on the specific scene. For example, Stroner et al. (2021) developed a method suitable for vegetation filtering on steep slopes from a point cloud derived by structure from motion (SfM) algorithms and tested it on railway ledges. Zhao et al. (2016) proposed an improved progressive TIN densification filtering method adjusted for usage in forested areas with steep slopes, where it outperformed the original progressive TIN densification method. A general description of two methods that are practically implemented for specific sandstone areas in this paper follows.
- **Spatially conditioned filtering.** This approach was applied for example by Trommler (2007) on a sandstone landscape point cloud. It is based on the assumption that the success rate of the filtering method in sandstone areas depends on the parameters of the settings. The area of interest is divided into classes, and for each class the filtering parameters are set differently. Steep rock faces form a separate category with less strict parameters for filtering, in order to keep the information about the edges of cliffs.

The limitation of this method is that there is a strong need for the data delimiting the classes to have an adequate level of detail and accuracy. For example, classification of an orthophoto where a rock taller than the surrounding trees is easily identifiable, may be employed for this purpose but it is not applicable for objects hidden under the canopy. Moreover, after filtering, problems with merging the data into a seamless DTM must be resolved. Implementation of this approach is proposed in Subsection 4.1.

- **Object-oriented classification.** The processing of laser scanning point clouds may be more robust when analysing objects rather than individual points (Sithole, 2005), similar to human visual interpretation of the point cloud. Segmentation needs to be carried out first. Various approaches to this task have been developed, e.g., region-growing-based segmentation with defined homogeneity and the spatial proximity of points is often used (Shan and Toth, 2018). Classification of individual segments is applied afterwards. The second proposed method makes use of this approach and invents features based on the distribution of the points within objects of the rock pillars and trees (Subsection 4.2).
- 4) **Filtering with support of terrain data.** Once time and resources have been invested in creating precisely filtered data from various types of terrain, another point cloud may be filtered with the support of the existing terrain data. The typical task is then to filter a denser point cloud using the existing sparser data from previous scanning. By using spatially conditioned querying, ground points from a denser point cloud are selected based on the spatial relationship with the ground points from the filtered point cloud. The preceding step is a precise co-registration of the point clouds that in principle is a similar task to the strip adjustment that has been already discussed. As the two point clouds generally do not include identical points, the matching is done based on the interpolated surface and point cloud, two interpolated surfaces, or two point clouds but with the extent restricted to simple shapes, most preferably planes (Shan and Toth, 2018). The transformation parameters are then derived by a registration algorithm, e.g., the commonly used iterative closest point (ICP; Besl and McKay, 1992). As calculating the algorithm is time consuming and complex, approaches with more effective computation are being developed, e.g., using singular value decomposition (SVD; Williams and Bennamoun, 2001) or matching corresponding points based on geometry features such as a curvature, point cloud density, or normals (GF-ICP; He et al., 2017). The particular implementation of the method adjusted to sandstone landscapes is presented in Subsection 4.3.

2.3. Available ALS datasets in Czechia

One of the first attempts to demonstrate the potential of ALS in a wooded sandstone landscape was made in March and April 1997 in the Saxon Switzerland National Park in Germany (50.92° N, 14.14° E). About 56 million laser points were collected with a density of about one point per 9 m² (Csaplovics, 2007). Experiments showed that an automatic approach to point filtering and classifications based on linear prediction allowed cliffs and rock plateaus to be separated to some extent. But in general, the resulting digital models displayed overly smoothed hill-like objects instead of rugged and steep rock walls and pillars. Further research dealt with the extraction of rock edges using high pass filtering and morphologic operators (Csaplovics et al., 2003).

The new campaign called GeNeSiS, which covers the whole sandstone area along the Czech-German border – both the Bohemian (50.88° N, 14.37° E) and the Saxon Switzerland National Parks (approximately 800 km²), was carried out in April 2005. In the following text, we will refer to this data as *NP data*. The mean point density of the last echo measurement was 8.5 points per sq. m. The first echo, the last echo, and the intensity of the last echo were recorded, and colour infrared and RGB imagery with a pixel size of 0.5 m was collected simultaneously. The TopoSys system Falcon II with optical fibres for emitting the laser pulses

was used (TopoSys, 2021). This is why a parallel wiggly or wavy pattern is noticeable in the point cloud (Fig. 4B). During the data processing, focus was put on keeping information about the topography of sandstone rocks. Acquired data were processed using hierarchical robust interpolation in SCOP++ software (Trimble, 2021a). The experiments showed that using only one filtering parameter for the whole area did not provide satisfactory results. Therefore, spatially conditioned filtering was applied. Two DTMs were computed with the first being optimised for building elimination (but smoothing the rocks) and the second for maintaining details in the rocky terrain (but not eliminating the buildings). The results were combined using polygons for delimiting the rocks. The polygons were manually digitised using hillshaded relief based on the second, rock-features-enhanced DTM. The information about intensity was not used for processing. The outcomes of the project included, among others, a DTM and digital surface model (DSM) with a resolution of 1 m, RMSE at a height of 0.38 m, and maximum errors rising up to 4 m in rocky areas on cliff edges (Trommler, 2007). Further research with acquired data was carried out. For example, experiments with filtering parameters and supporting information from aerial imagery in TerraScan software (TerraSolid, 2021) were performed to enhance the modelling of rocks, as published in Gašior (2006).

A nationwide LiDAR mapping of Czechia was performed between 2010 and 2013 by the Czech Land Survey Office, including all sandstone landscapes within its territory. In the following text, we will refer to this data as *LSO data*. The flight altitude was approximately 1200 m above the average elevation of terrain with a 50 % overlap of scanning strips, and the mean point density reached approximately 1.5 points per sq. m (Dušánek, 2014; Fig. 3A). Using a RIEGL LMS Q680 airborne laser scanner with a rotating mirror, the echoes had a linear pattern (RIEGL, 2021; Fig. 4A). Full-waveform information about the reflected echoes was recorded but was not applied in creating any of the final products. The raw data were processed using SCOP++ and DTMaster (Trimble, 2021b) and subsequently thoroughly manually checked and corrected. There are a few final products, the most relevant for the following text is the nationwide digital terrain model of the 5th generation (DMR 5G). It consists of irregularly distributed 3D points, forming nodes of a triangulated irregular network (TIN). Currently, this model represents the most accurate elevation data covering the whole territory of Czechia with RMSE at the height of 0.18 m in bare terrain and 0.3 m in terrain covered by dense vegetation (Dušánek, 2014). The usability of DMR 5G and LSO data (before filtering) for mapping of rock formations is discussed in Paleček and Kubíček (2018). Even though the point density of LSO data is noted as being too low (10 points per sq. m is suggested as a minimum), the DTM derived by precise filtering is considered promising for identification of medium-sized rocks.

In April 2008, before the nationwide mapping of Czechia, a test scanning with a RIEGL LMS Q680 scanner was executed in the Prachov rocks in the Bohemian Paradise region (50.47° N, 15.29° E). The flight altitude was also about 1200 m above the terrain and the overlap of neighbouring strips was set to 40 %. The resulting point density was 1.2 points per sq. m with RMSE of the elevation better than 0.1 m (Fiala, 2011). Other experimental data were acquired by the Czech Land Survey Office in November 2013 in the Adršpach-Teplice Rocks (50.60° N, 16.13° E). For more detailed capturing of the rock cities, the flight altitude was about 900 m above the terrain, the overlap of neighbouring strips was 40 % and, most importantly, the flight strips were arranged in two perpendicular flight directions to eliminate the occluded areas behind the rock pillars. The mean point density of the resulting point cloud reached 4.5 points per sq. m (Fig. 3B), and the density of the last echoes 3 points per sq. m. These data are referred to as *AT LSO data* in the following text.

3. Study areas

The experiments presented in the following sections were tested on point clouds from two sandstone regions in Czechia, i.e., the Bohemian

Switzerland National Park, and the Adršpach-Teplice Rocks in the Broumovsko Protected Landscape Area. The following text briefly describes the regions and the rock formations that may be found there. Particular locations of interest with additional information, such as coordinates, size, specific formations, and visualisations of the terrain may be found in the Appendix.

The Bohemian Switzerland National Park was established to protect the most unique part of the Elbe Sandstones area in the north-west part of the Bohemian Cretaceous Basin. The massive sandstone deposits that enabled for the development of plateaus, deep canyons, and various meso- and micro-forms exist on both sides of the national border. In Germany, the Saxon Switzerland National Park has been declared to protect this area. The landscape is divided into three height levels, the lower one forming deep river canyon (the Elbe River Canyon) and valleys, the middle one constituting a structural plateau, and the upper one consisting of table mountains and rock cities (Vařilová, 2016). The most famous rock formation in the park is the Pravčická brána Arch (Prebischtor in German; Fig. 5A, Fig. 5B), which is the largest natural sandstone arch in Europe. It is located in the upper height level and is surrounded by imposing rock walls of a height of tens of metres. A more detailed description of the region may be found for example in Cílek (2010), Vařilová (2016). Development and anthropogenic impact on the Pravčická brána Arch is the subject of a study by Vařilová et al. (2015).

The Adršpach-Teplice Rocks are situated in north-eastern Bohemia and are protected as a part of the Broumovsko Protected Landscape Area. They represent the most extensive complex of sandstone formations constituting a rock city in Czechia (Mikuláš et al., 2007). The area is split into two parts by a natural border created by the Vlčí rokle Gorge. The smaller part in the north is called Adršpach Rocks and represents a typical rock city with narrow gorges and high pillars. The two most famous rock formations showing the late stage of erosional processes are *Milenci* ("Pair of Lovers"; Fig. 5C) and *Starosta a Starostová* ("Mayor and Mrs. Mayor"). The larger part in the south is called Teplice Rocks and its dominants are massive rock walls and dissected plateaus (Fig. 5D). A broader description of the area may be found for example in Vítek (2016).

4. Improved filtering methods for sandstone landscapes and their evaluation

Filtered ALS datasets from different sandstone landscapes (Subsection 2.3) obtained by utilising the conventional filtering approaches described in Subsection 2.2 were visualised and areas with considerable filtering errors were identified and analysed. Based on that, three experimental filtering methods adjusted to these specific areas were developed. Spatially conditioned filtering and object-oriented classification are two approaches suited for geomorphologically distinct regions, i.e., reliefs with rather compact rock walls, and plateaus and areas with dominating rock pillars and trees, respectively. The third approach uses already existing filtered terrain data and can be considered as rather general, independent of specific relief type and applicable also on other terrains. Its limitations are in the availability of filtered terrain data with a suitable resolution or point cloud density.

The following subsections describe the proposed methods in detail, and the results of their experimental implementation and testing. The evaluation is presented in two ways, statistical and visual. While the statistical evaluation may objectively quantify the success rate of the methods, the visual interpretation is beneficial for describing the spatial distribution of misclassified points, or inaccuracy in the resulting point cloud. For a quantitative analysis, ground truth data are essential. In the case of object-oriented classification, manual point cloud filtering was carried out to obtain data that may be considered as ground truth. For evaluation of the other two methods, in situ geodetic measurements or an existing filtered point cloud were employed (Table 1).

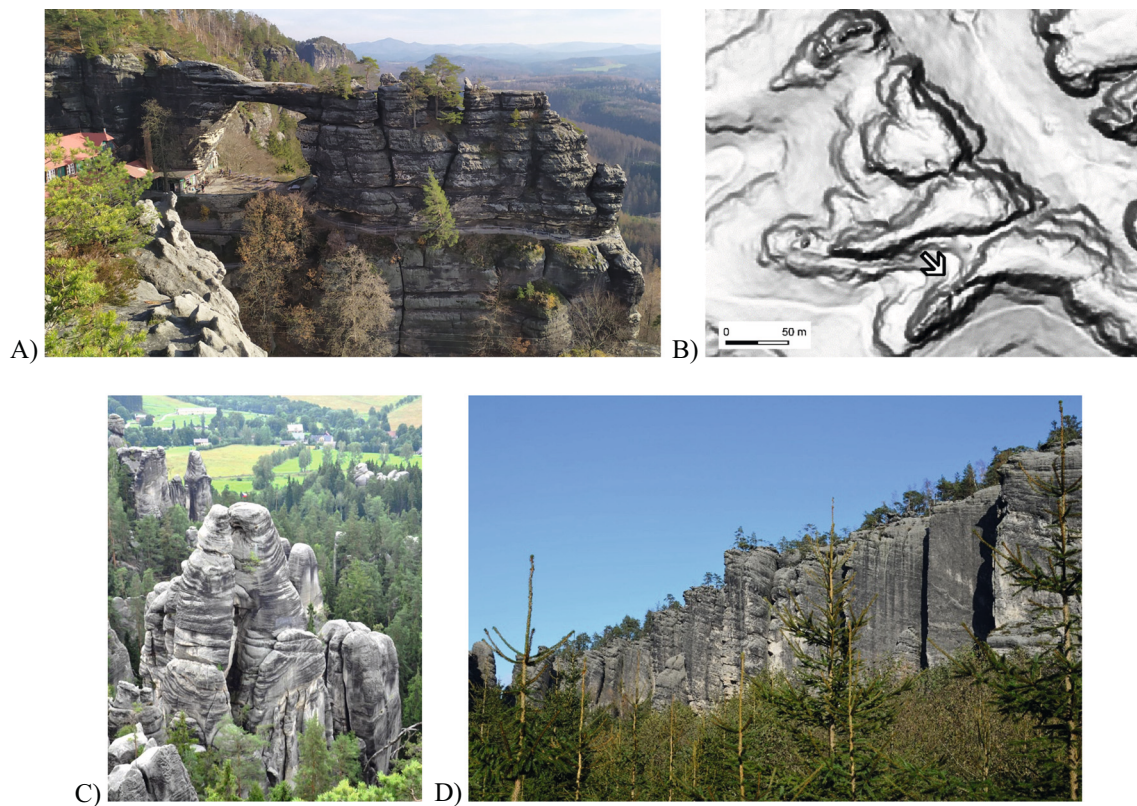


Fig. 5. Locations of interest. A) The Pravčická brána Arch captured from the neighbouring rock cliff that is accessible to tourists. B) Hillshaded visualisation of the filtered NP data around the Pravčická brána Arch (arrow). C) Milenci rock formation in the Adršpach Rock City. D) The Martinské stěny Walls in the Teplice Rock City.

Table 1

Overview of data used for testing and evaluating the proposed methods. Filtered data refers to data filtered in the scope of projects carried out by other institutions as described in Subsection 2.3, except for data filtered by the LAStools *lasground* function (one of the conventional filtering methods) and manually filtered data that have been filtered for the purpose of this experiment. See the Appendix for more details about the localities.

Method	Testing data	Reference data	Locality
Spatially conditioned filtering	LSO data	Filtered NP data and LSO data filtered by <i>lasground</i>	Bohemian Switzerland (NP A and NP B)
Object-oriented classification	Merged LSO and AT LSO data	Manually filtered merged LSO and AT LSO data, filtered LSO data, and LSO data filtered by <i>lasground</i>	Adršpach-Teplice Rocks
Filtering with additional terrain data	NP data with support of filtered LSO data	Filtered NP data, filtered LSO data and GNSS measurements	Bohemian Switzerland (NP C)

4.1. Spatially conditioned filtering

Spatially conditioned filtering is an iterative method consisting of two main steps, defining zones of relief with similar characteristics and applying filtering with adjusted parameters on these zones. A similar approach was previously used for processing data in the GeNeSiS project (see Subsection 2.3). Since the zones and parameters for filtering in the GeNeSiS project were defined manually, our aim was to automate and optimise the process. Another difference lies in the definition of zones with rocks. As the most problematic parts for the filtering are the steep parts of rock formations such as walls (Fig. 6), the zones with rocks are restricted to an extent of the very steep terrain. Less rough terrain and flat sandstone plateaus are excluded, being filtered with a standard set of parameters. Due to this fact, the method is applicable in areas with prevailing large-scale rock structures, such as parts of the Bohemian Switzerland National Park, but is not suitable for very dissected terrains.

The automatic delineation of the zones with rocks is based on slope calculation and its thresholding in two iterations. Firstly, filtering of the point cloud is done using the *lasground* function from LAStools

(Isenburg, 2020). LAStools is a library of functions for processing of point clouds and *lasground* is a standard filtering method based on the TIN densification method (Axelsson, 2000). The objective of this step is to provide a rough estimation of the ground; therefore, parameters are set to eliminate all vegetation, which also eliminates lots of points

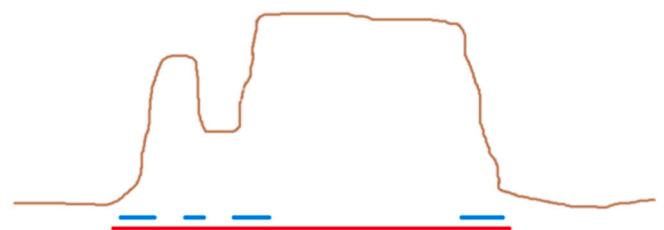


Fig. 6. Different classifications of zones with rocks. In the GeNeSiS project, entire rock structures were included in the zones with rocks (red line). In contrast, the proposed method classifies only steep parts of the rocks as zones with rocks (blue line). (For interpretation of the references to colour in this figure legend, the reader is referred to the web version of this article.)

belonging to rocks. The generated TIN serves as an input for slope calculation. The slope is thresholded with hysteresis, whereby zones with a higher slope than the threshold and their adjacent zones with slope higher than the lower threshold are perceived as potential zones with rocks. This strategy prevents isolated areas of relatively low slope from being selected and at the same time, preserves parts of rocks that are not so steep. An additional generalising feature lies in the evaluation of the ratio of potential zones with rocks within a grid of an adjustable cell size. Only cells with a ratio that surpasses the threshold are further processed.

The second iteration aims to refine the shape of zones with rocks. Within the selected grid cells, the original point cloud is filtered again by the LAsTools *lasground* function but with less strict parameters than in the previous step. Then, the slope calculation and thresholding are executed identically as before. Finally, the potential zones with rocks are filtered based on their size to avoid including residual vegetation that may cause higher slopes in small areas.

The spatially filtered method was evaluated using filtered NP data on two subsets of the Bohemian Switzerland National Park denoted NP A and NP B. Locality NP A contains the town of Janov and Kamenice canyon. The landscape in this locality is quite flat, except for Kamenice canyon. Locality NP B includes the Pravčická brána Arch with surrounding rock walls and other features of sandstone relief, and a flat part only in the south. For more detailed information about the locations see the [Appendix](#).

The first part of the evaluation of the proposed method focused on the delineation of zones with rocks. Based on visual evaluation, the limit for the slope representing rocks was set to 42° and the lower threshold applied on adjacent areas was 35° . To capture the influence of parameters on the resulting zones, multiple sets of crucial parameters were tested, including a grid size (100–400 m), a proportion of potential zones with rocks in each cell (5–20 %), and a step parameter in the second iteration of filtering using the *lasground* function (3–5 m). The final selection (grid size of 400 m, proportion of zones with rocks of 9 %, and step of 3 m) is made based on the visual interpretation as well as an evaluation of the computational effort because the smaller size of the cells in the grid dramatically increased the computational time.

Differences in the delineation of zones with rocks may be observed between the two locations of interest. With the increased step parameter, some rock features became too small to be present in the filtered terrain. Due to this fact, the increased step parameter caused a decrease in zones with rocks in the locality NP B. In the locality NP A, where most of the rock formations are located on the slopes of the canyon, the influence of the increasing step parameter was negligible because the slope between the surrounding terrain (the upper and lower part of the canyon) is sufficiently high even without some smaller rock features.

In the second part of the evaluation, we compared three terrain models, i.e., filtered NP data, LSO data filtered with just one set of filtering parameters without zoning, and LSO data filtered with two sets of parameters applied on delineated zones. The parameters for filtering the LSO data were determined by a grid search optimising RMSE with respect to the NP data. In both locations of interest, the spatially conditioned filtering achieved lower RMSE than the filtering with one set of parameters ([Table 2](#)).

The visual outcomes of filtering capture the distribution of inaccuracies in both locations. In locality NP A, the filtering with one set of parameters filtered out most of the canyon walls and did not eliminate

the vast areas of vegetation in and around the canyon ([Fig. 7A](#)). In general, the spatially conditioned model better maintained the slopes of the canyon, but also filtered out parts of rock features, and did not remove large areas of vegetation in the less rough parts of the locality, although these areas are significantly smaller than in the case of the previous model ([Fig. 7B](#)). In locality NP B, the results may be interpreted similarly, whereas filtering with one set of parameters did not preserve the rocks well, nor did it remove vegetation ([Fig. 7C](#)). Spatially conditioned filtering smoothed the edges of rocks in some cases more so than in the first version because zones were imprecisely delineated. However, in these places, it mainly reduced the difference in height compared to the NP data and kept significantly less vegetation in both zones with and without rocks ([Fig. 7D](#)).

4.2. Object-oriented classification

The proposed object-oriented classification method is inspired by the procedure of manual classification, whereby an expert operator recognises the rock pillar and tree based on the distribution of points inside the object, e.g., rock pillars are hollow while trees usually contain irregularly distributed points, which come from branches and leaves. Therefore, the method is fitted to the scale of formations in the rock cities rather than large-scale rock structures. The essential assumption for the success of manual classification (and of the described method) is a sufficient point cloud density ([Fig. 3](#)). The lower limit of usable density depends on the size of the objects that need to be recognised. Based on our experience, a few points per sq. m (5–10 points per sq. m) are sufficient for the classification of most of the standard-sized pillars, but distinguishing between smaller formations in the terrain, e.g., those covered by spruce grove and high ferns, is not reliable.

The method may be described in three steps. Firstly, segmentation of an approximate surface on top of the point cloud divides the point cloud into objects. In the second step, these objects are classified using features describing the inner distribution of points to classes of rocks, trees, and a mixed class. Finally, the trees and mixed classes are filtered with relatively strict parameters, while the rocks are left without additional filtering. This step is in principle similar to the spatially conditioned filtering, but scale plays a role in this case. Also in this case, zones for finer filtering are whole medium-sized formations, while the spatially conditioned filtering focuses on a part of large-sized features.

The idea of the segmentation lies in the fact that rock pillars and trees create elevations in the surrounding terrain. The approximate surface on top of the point cloud is interpolated by a spline with tension from the points with maximal height in a cell of a grid of an adjusted size. The purpose of using a spline is to create a smooth surface with minimal curvature that exactly reflects the height of points, and the tension ensures that the spline does not considerably fluctuate. To find local minimums that divide the surface into the intended objects, a watershed segmentation is applied on the reverse surface where the rocks and trees are represented by sinks and the division lines between objects define the basins ([Beucher and Lantuéjoul, 1979](#)). Post-processing of the segmented objects is required due to over-segmentation of pillars with more peaks at the top. To merge the neighbouring objects that belong to one pillar (or possibly also a tree), a criterion of the relative height of the border is introduced. This criterion reflects the need to merge relatively high objects with low borders. An illustration of this situation is included in [Fig. 8](#). To avoid merging too many objects, the threshold is set to 10

Table 2

Comparison of RMSE between filtering with one set of parameters and spatially conditioned filtering, applied on an LSO dataset and the filtered NP data in the locations of interest.

Filtration	NP A [m]	NP B [m]	NP A + B [m]
One set of parameters	1.55	2.89	2.31
Spatially conditioned	1.23	2.38	1.86

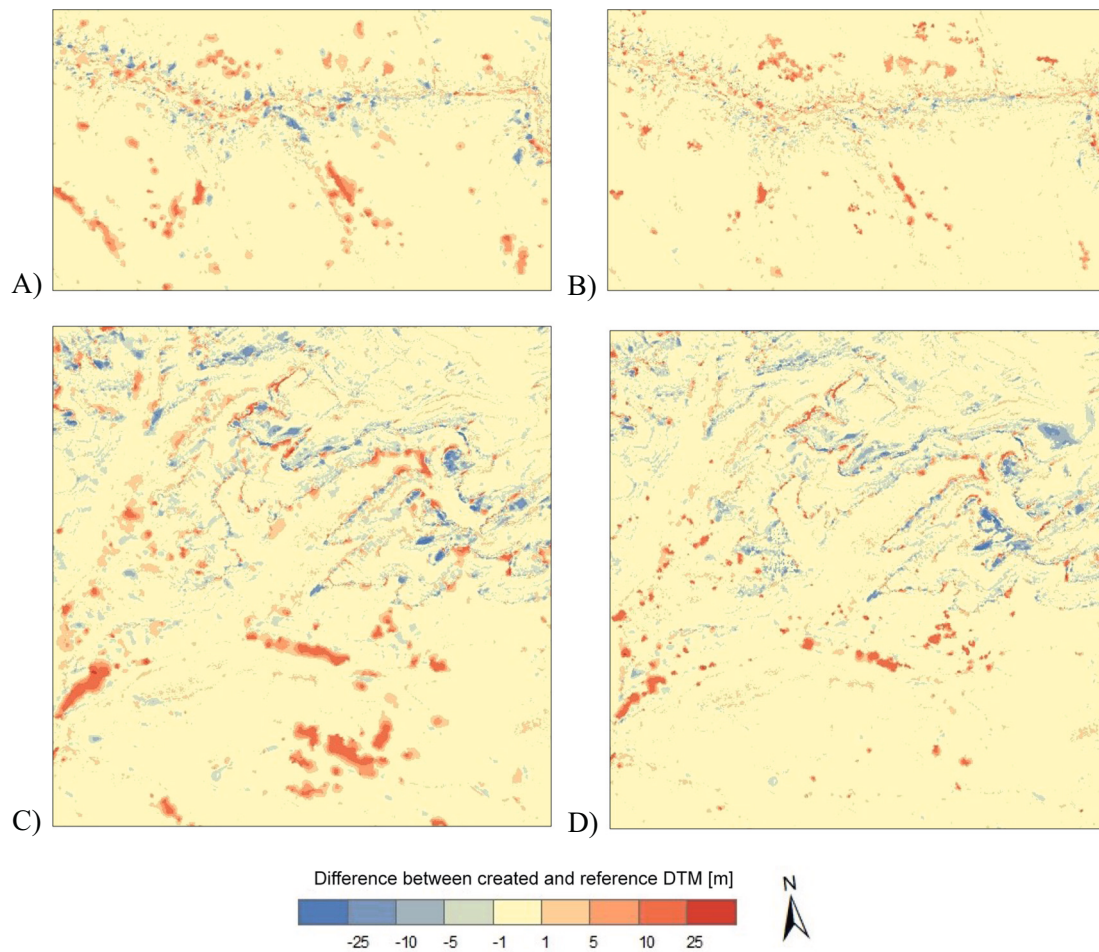


Fig. 7. Visual comparison of the results of filtering with one set of parameters and filtered NP data (A, C) and spatially conditioned filtering and filtered NP data (B, D) in locality NP A (A, B; clipped to $2 \times 1 \text{ km}^2$) and NP B (C, D; $2 \times 2 \text{ km}^2$).

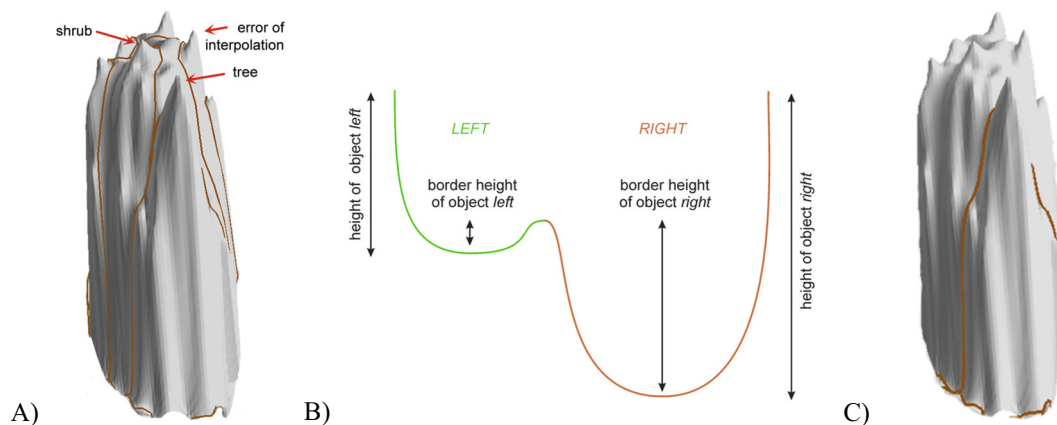


Fig. 8. Post-processing of segmented objects. An example of an over-segmented rock pillar (A) due to various reasons – shrub, tree growing on the pillar, interpolation error. Brown lines represent borders of the segmented objects. An inverse surface with two objects for illustration of criterion for merging neighbouring objects (B) – if the proportion of height of border with the neighbouring object to overall height of the object is lower than 10 % (fulfilled for the *left* object, not for the *right* object), then the object is merged with the neighbouring one. An example of the rock pillar after post-processing (C) – it remains divided into two parts due to a relative high tree growing on the pillar but with the other objects merged to one object representing the main part of the rock pillar. (For interpretation of the references to colour in this figure legend, the reader is referred to the web version of this article.)

% . The post-processing is performed in iterations because after each iteration new objects with new parameters are created.

In the next step, features reflecting the inner-object point distribution are calculated to be used as an input to the classification. Each

object is cut by three horizontal planes into a quarter, half, and three quarters of the object height, and points below each the horizontal plane are considered. The assumption that the rock objects have very low point density inside compared to the border, while the tree objects have

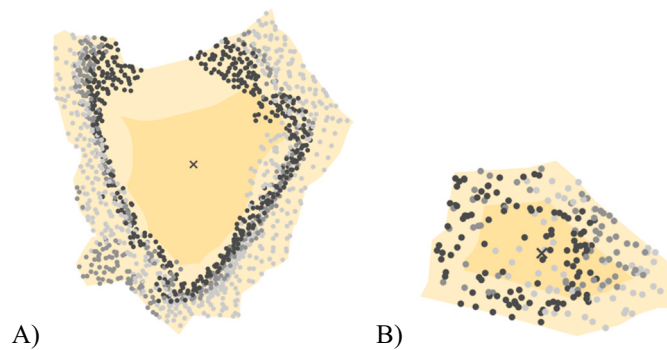


Fig. 9. Projection of points within the cuts on the horizontal plane (the lighter grey, the lower cut) and delineation of inner and outer zones - darker and light brown polygons, respectively. The rock formations tend to have most of the points in the outer zone (A) while in the case of trees, the distribution of points within the cuts and zones is similar (B). (For interpretation of the references to colour in this figure legend, the reader is referred to the web version of this article.)

similar values of both is reflected in the features of the point density in the outer and inner zones of each cut (Fig. 9). The line dividing the inner and outer zones is defined by a buffer with a radius of half of the shortest distance between the object boundary and the centroid. Because the assumption is based on well-shaped features, more robust features are added, whereby creating an absolute and relative area without points within the cut. The area is derived from a 1-m grid as the largest continuous area without a point. As a classification algorithm, a decision tree is used due to its straightforward interpretation as a set of rules based on selected features that have significant distinguishable properties. The target classes are specified as rock, tree, and mixed for those objects where both previous classes are covered and cannot be divided (e.g., a tree growing on the top of a pillar).

The last step of the proposed method is filtering conditioned by the class of the object. In the case of the rock class, all points are labelled as ground points. In other cases, the filtering algorithm implemented in the function *lasground* from LAStools with different values of the offset parameter is used. For objects of the tree class, the offset is set to 1 to avoid misclassification of non-ground points within a class where all higher points should be vegetation. In contrast, the offset is set to 5 in the case of the mixed class to prevent rocks being filtered out.

To evaluate the method, 11 areas with varying morphological conditions and vegetation coverage were defined in the Adršpach-Tepliče Rocks (see the Appendix). The point cloud created by merging LSO and AT LSO data from these locations was manually filtered and the results were verified in the field. Points for interpolation were determined from a $2 \times 2 \text{ m}^2$ grid, which was adjusted to a point density of the merged data of 7 points per sq. m. In the classification trialled using data from the Milenci location, only four features were selected as relevant to distinguish the classes, i.e., the absolute area without points within the lower cut, the absolute area without points within the middle cut, the relative area without points within the upper cut, and the outer-zone point density of the middle cut.

In comparison to the manually filtered data, the overall accuracy of the output from the proposed method reaches 85 % in total for all the

locations of interest. As may be seen from the error matrix (Table 3), about 20 % of the ground points were filtered out. In contrast, only 9 % of the vegetation points were assigned as ground points, so the number of false positives is significantly lower than false negatives. Both conventional filtering methods achieved a lower percentage of correctly classified points, i.e., 78 % and 70 % in the case of the filtered LSO data and the LSO data filtered using the *lasground* function, respectively. The proposed method corresponds to the filtered LSO data by 80 %, but the LSO data filtered out approximately half of the ground points despite the manual correction after the application of robust interpolation (for details see Subsection 2.3). The main differences between the proposed method and the *lasground* results are in the objects of the rock class that results from the methodology, i.e., in the final step, classes other than rock are filtered by the proposed approach.

The distribution of misclassified points may be even more important than the mentioned accuracy metrics in this case. The aim of the method is to retain points of rock formations in the filtered point cloud to serve as an input for DTM generation and mapping purposes. Fulfilling this requirement depends on the location and its conditions. See Fig. 10 for the visual comparison of DTMs created from filtered data for the Milenci location. In the results of the proposed method, a few very narrow rock needles were filtered out at this location. These needles are so close to the trees that the segmentation was not able to differentiate the two objects in the point cloud. The resulting joined object was classified correctly as the mixed class, but the final filtering was not able to filter out the tree and leave the needle when they were so close to each other (Fig. 11). Another case of filtering a rock pillar out from the ground appeared at the Labyrinth location. The height of the pillar was over-estimated due to the vegetation at the top, so the upper cut was made on the part where the wall changes to the top platform. Due to this, together with an overhang at the bottom of the pillar, points are distributed almost uniformly in the upper cut and therefore the area without points is too small. Additionally, the variety of morphological features and shapes in the locations of interest may also contribute to insufficient results. For example, locations at the Skalní ostrov Plateau are primarily formed by a solid platform gradually turning on the edges into high rock pillars with very narrow chasms in between. These objects do not represent features suitable for the proposed method because the segmentation is not able to distinguish between them or to distinguish them from other objects at the top of the platform.

4.3. Filtering with additional terrain data

Filtering with additional terrain data requires two data sets as the input, i.e., the point cloud that is to be filtered (*input data*), and the terrain data (*reference data*). Reference data may be either another point cloud that was already precisely filtered or a raster DTM derived from it. In the following text, the use of a filtered point cloud is described. The method consists of two main steps with a third that is beneficial in our experiment but may not be useful or even possible in other cases. The first step includes a precise co-registration of data sets, which is complicated in rough terrain covered by vegetation, as discussed in Section 2. The approach is based on the employed data; therefore, our workflow is described below together with the used data and obtained results. The co-registration is essential for the next step in which the filtering itself is executed by using spatially conditioned querying. In the

Table 3
Error matrix comparing the results of the proposed method (rows) and manual filtering (columns).

	Ground	Non-ground	Total	User's accuracy
Ground	123,064	9940	133,004	92.5 %
Non-ground	29,529	106,718	136,247	78.3 %
Total	152,593	116,658	269,251	
Producer's accuracy	80.7 %	91.5 %		85.3 %

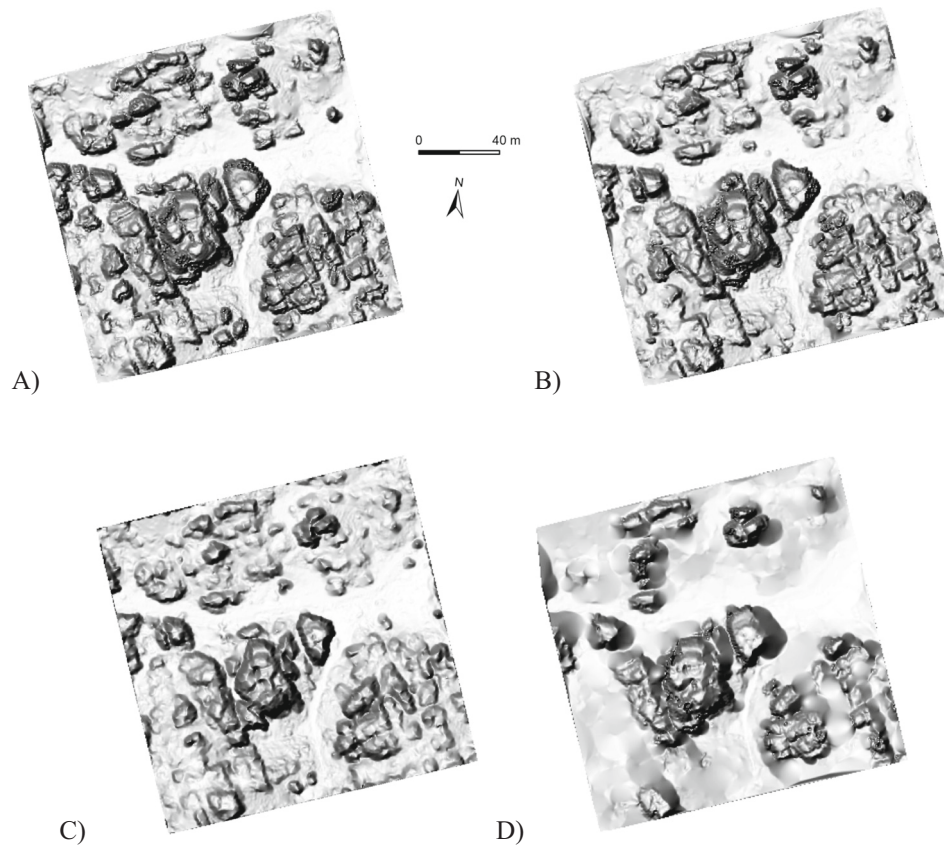


Fig. 10. Visualisation of all the compared filtering methods for the Milenci location applied on LSO data – A) manual filtering, B) the proposed method, C) *lasground* from LAStools, D) the originally filtered LSO data.

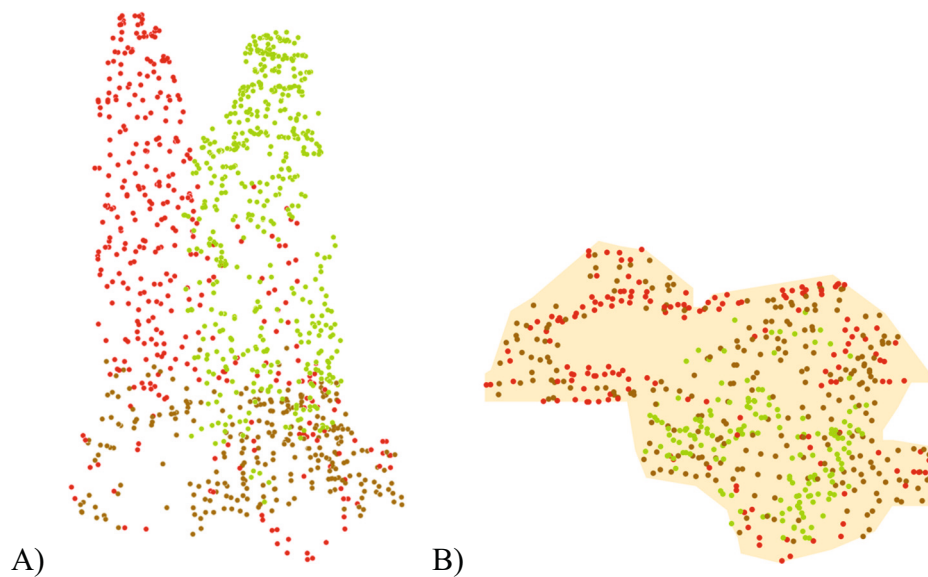


Fig. 11. Incorrectly classified rock pillar. Visualisation of one the objects of the mixed class – A) 3D view, B) the middle cut of the object. The green points represent a tree, brown points the ground, and red points the rock pillar that was filtered out. (For interpretation of the references to colour in this figure legend, the reader is referred to the web version of this article.)

case of a low density of reference data with respect to the highly variable relief, the additional step is designed to locally improve the filtering with the employment of automatically filtered input data.

An illustration of spatially conditioned querying is shown in Fig. 12A. As both point clouds are irregularly sampled, it is beneficial to

create a continuous surface from the reference data and compare it to the points that are to be filtered. The surface used in our case consists of a triangulated irregular network (TIN) but other interpolation methods (e.g., linear interpolation, inverse distance weighting) may be applied as well. The spatially conditioned querying is set as follows:

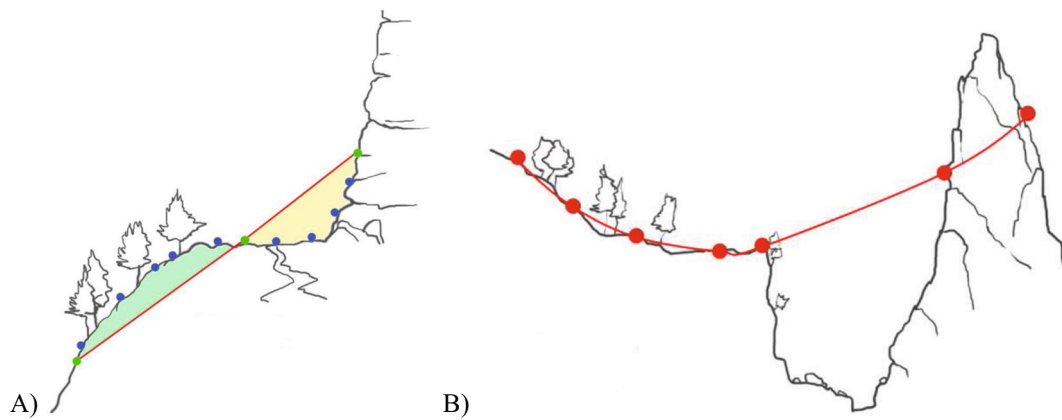


Fig. 12. Illustration of spatially conditioned querying on LSO data (green points and red line) and NP data (blue points) (A). Illustration of the situation with missing points in the valley due to a low density of the point cloud (B). (For interpretation of the references to colour in this figure legend, the reader is referred to the web version of this article.)

Table 4

Comparison of DTMs derived from ground points filtered by the proposed method with varying distance tolerance parameters and filtered NP data and filtered LSO data. Negative values mean that the created DTM is above the filtered LSO data.

	Filtered NP data		Filtered LSO data	
	Average height difference [cm]	RMSE [m]	Average height difference [cm]	RMSE [m]
DTM (15 cm)	48.0	2.457	-36.6	2.302
DTM (35 cm)	49.7	2.480	-34.8	2.295
DTM (50 cm)	52.0	2.489	-32.6	2.290

- $Z_{value} \leq (surface + threshold) \rightarrow terrainpoints$
- $Z_{value} > (surface + threshold) \rightarrow offterrainpoints$

The querying may be repeated with already classified ground points as part of the interpolated surface but with more iterations, the ground “climbs up” on vegetation.

In the case of using a point cloud with low density as the reference data, the additional step of improving the filtering may be useful. The situation that may occur locally is shown in Fig. 12B. The density of reference data is so low that there are no points in the valley. According to the approach mentioned above, all points below the surface are considered ground points. If there is vegetation at the bottom of the valley, it is misclassified. Such locations are identified by the thresholding ratio of ground and non-ground points per triangle in the TIN and then filtered in the same way as described above but with a different surface, this time using automatically filtered ground points by means of another method (e.g., TIN densification or robust interpolation) applied to the input data. Even though the automatic filtering smooths rough terrain, in the case of a sufficiently dense point cloud, there may be some points at the bottom of the valley that help with the filtering of vegetation.

For the presented experiment, we employed LSO data as reference data because they have been filtered and manually corrected. The input data to be filtered are NP data that are denser (more than 8 points per sq. m) compared to the LSO data (1.5 points per sq. m). Another difference between the data sets is in the distribution of points - LSO data have a

regular distribution, but the NP data set was captured by a scanner with optical fibres and therefore the distribution shows a wavy pattern (Fig. 4). The subset of NP data for the location of interest (NP C - see the Appendix) has approximately 1.33 million points, whereas the LSO data consist of 293 thousand points, from which only approximately 61 thousand were classified as ground points. Such a low proportion of ground points is caused by gathering the LSO data in July 2010, i.e., in the leaf-on season when the leaves prevent the pulses from reaching the ground. From this point of view, LSO data are not fully suitable for this purpose.

The co-registration of point clouds was executed using 23 localities, including well-observable objects in both point clouds. Cropped point clouds were manually filtered and ground points were compared location by location using the CloudCompare software (CloudCompare, 2021). The derived transformation matrices were evaluated by cluster analysis (in our case a dendrogram) to eliminate bias by non-precise manual filtering and other factors. Only 12 locations with similar transformations were selected, and the final transformation matrix was calculated as a mean of the observations per location. Finally, as none of the point clouds may be considered more precise with respect to the absolute coordinates, both point clouds were translated and rotated by half of the transformation matrix in opposite directions. By using the described approach, the mean deviation of height among points within the point clouds decreased almost by half (from 31.7 cm to 16.8 cm).

The results of the proposed method are influenced by the parameter of the distance tolerance of points above the surface that are accepted as

Table 5

Comparison of all DTMs with geodetic measurements.

DTM	RMSE for all points [m]	RMSE for selected points [m]
DTM (15 cm)	1.706	0.472
DTM (35 cm)	1.385	0.470
DTM (50 cm)	1.386	0.471
Filtered LSO data	2.478	0.550
Filtered NP data	2.358	5.068

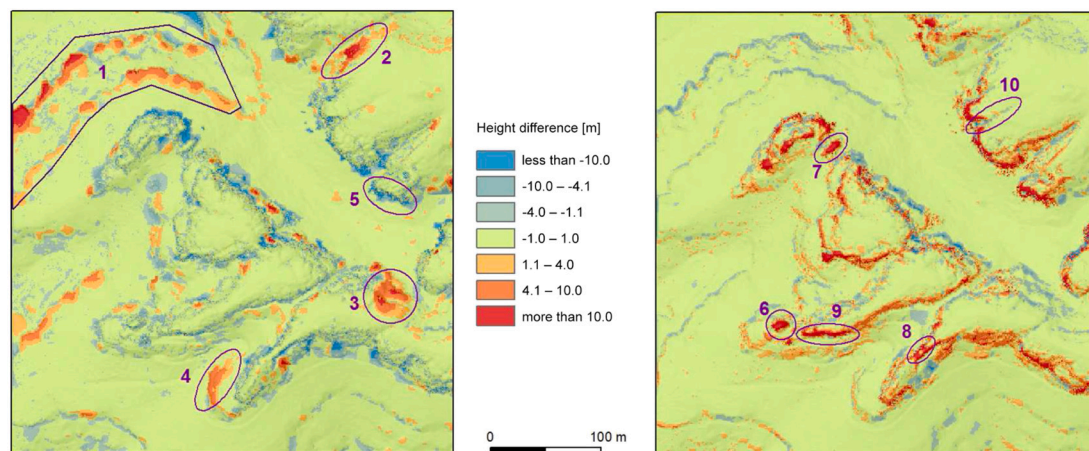


Fig. 13. Comparison of the created DTM (35 cm) with the filtered LSO data (left), or the filtered NP data (right). Explanation of the highlighted areas is in the text.

ground points. For the purposes of the experiment, the ground points were calculated using three values of the distance tolerance parameter, i. e., 15, 35, and 50 cm. The higher the parameter, the more the resulting ground climbs up along the vegetation. On the other hand, the parameter cannot be too low in such varying terrain because the rock formations would be filtered out.

For the evaluation of the proposed method, filtered LSO data, filtered NP data, and geodetic measurements in the central area of the location of interest were employed. To quantify the differences of the digital terrain models (DTMs), average height difference and RMSE were calculated (Table 4). The differences in height between DTMs are significant, with the highest differences being between the NP data and LSO data and the results of the proposed method being between these two DTMs. All the DTMs were compared to the geodetic measurements both separately for all 865 measurements, and for the subset of 25 points that lies at the edge of rock platforms on the highest parts of the rocks (Table 5). If we consider the geodetic measurements a ground truth, the best DTM is the result of the proposed method with a tolerance of 35 cm. The outlier in the measurements is the DTM from filtered NP data that achieves RMSE at the edges of rock platforms of more than 5 m. The explanation for this, as well as for the significantly better results for filtered LSO data, comes from the visual interpretation that will be described further in the next paragraph.

The visual interpretation and distribution of the differences between DTMs may be seen in Fig. 13. The highest variance is connected to the rock features in both cases. The DTM from the NP data underestimates the edges of the rock platform of the highest rock level (e.g., area 9 in Fig. 13) and distorts gorges in the platform (e.g., area 10). Filtered LSO data are more precise in these areas probably because of the manual correction that was made after the automatic filtering (area 5). The operators were able to recognise the rocks because the edges are often not fully covered by dense vegetation preventing echoes from reaching the ground. The drawbacks of the NP data classification are even more evident in the cases of two rock pillars and the Arch, whereby Erich's Pillar was fully filtered out (area 7), the Pravčický Pillar was 20 m lower than it should be (area 6), and the Pravčická brána Arch was divided into two parts without the arch between them (area 8). On the other hand, filtered LSO data smooth the lower levels of rock formations more than the DTM from NP data because they are located in the valleys covered by trees, so the density of LSO data is insufficient to distinguish rock formations from the terrain (area 1, 2, 3, and 4).

5. Discussion

In this study, we have proposed three filtering algorithms that may be considered as more suitable and reliable than conventional methods

applied on ALS point clouds in sandstone landscapes. The methods are adjusted to specific terrain in Central Europe. Filtering with additional, already existing terrain data is the most general method that is scalable to other types of landscapes, and not only sandstone. Object-oriented classification and spatially conditioned filtering are methods designed for very specific scenes. Object-oriented classification reflects the similarity of trees and rock pillars in rock cities, and efficiently distinguishes between them thanks to features capturing point distribution inside these objects. It is not applicable to larger scale rock outcrops because definition of the objects relies on the idea that trees and rock pillars create elevations in the surface that may be identified by a watershed algorithm. For rock plateaus, this assumption is not fulfilled. For larger-scale features, spatially conditioned filtering is suggested.

An evaluation of the improved filtering methods was performed with ground truth, if available, or as a comparison with datasets filtered by conventional methods. Due to the fact that the spatial distribution of the errors is terrain dependent, visual inspection was inevitable. Spatially conditioned filtering provides lower RMSE than filtering with one set of parameters, both comparing a dataset filtered by spatially conditioned filtering with manually selected areas, as described in Trommler (2007). The proposed method reached similar results with differences that cannot be described as advantages or disadvantages without proper ground truth data that are not available in this area. One unquestionable advantage is in the automation of the process of delineating zones for the application of the specific sets of parameters, which speeds up the filtering process and reduces the costs connected with the filtering. The need to search for the optimal parameters still remains.

Object-oriented classification outperformed the conventional methods in comparison with manually filtered ground truth data. The dataset reached an overall accuracy of 85 % but filtered out a significant number of ground points. As discussed in (Sithole and Vosselman, 2004), this type of error is also typically higher for conventional methods because, in general, there is a tendency to minimise non-ground points in the ground (an opposite type of error). The cost of leaving a significant number of non-ground points in the ground is considered to be higher because these points create non-existing shapes in the final DTM. It is difficult to compare the performance metrics of the proposed method with methods described in other published studies due to the different characteristics of the areas that they were applied on. According to the findings described in Zhao et al. (2018), slopes are a very important factor and source of errors, especially with respect to misclassified non-ground points. In comparison with the results of this study, where the filtering methods were applied on areas with slopes up to 40°, object-oriented classification yielded better results than most of the filtering methods in terms of the overall accuracy and both types of errors.

On the one hand, filtering with additional terrain data represents the most general proposed method but on the other hand it depends on the existence of a suitable DTM that supports the filtering of new point clouds. Comparison with geodetic measurements from the field showed that the DTM developed using this method outperformed the DTM created from the same input data but with the use of the spatially conditioned filtering described in Trommler (2007). The significant differences in the DTMs are in the edges of rock plateaus. Trommler (2007) reported RMSE on edges of sandstone massifs up to 4 m but based on our measurements, the RMSE is higher (more than 5 m). The model developed with the proposed method reached even lower RMSE than the DTM that was used as a reference in the method (0.47 and 0.55 m, respectively). This may be due to the higher density and accuracy of the filtered point cloud. Generally, the output DTM will reflect the problems of the reference one, e.g., if there is a missing rock pillar in the reference DTM, then with a high probability it will also be missing in the resulting DTM; however, it may improve the accuracy of local features like edges or valleys, especially if the new point cloud is of a higher density and/or accuracy.

Research of filtering extreme or edge-case terrain and situations is still topical. Most studies focusing on the performance of the filtering methods report that filtering on steep slopes, vegetated areas, and scenes with similar characteristics, such as sand dunes on the coast, yields unsuccessful results (e.g., Sithole and Vosselman, 2004; Zhang and Whitman, 2005; Zhao et al., 2018). We have shown that by adjusting the filtering methods it is possible to filter high-energy, vegetated terrain. We are aware that such an approach is limited to the specific type of terrain. It requires good knowledge of the ALS data and processing procedures, as well as characteristic features of the terrain itself when selecting an optimal filtering method and modifying its parameters. At the same time, such approaches have not been surpassed yet. Nevertheless, we believe that addressing the problems and providing solutions suitable for specific types of terrain will contribute to the future development of complex filtering approaches adaptable to terrain variability.

6. Conclusions

The sandstone landscapes in Central Europe comprise a variety of rock formations covered with vegetation of diverse height and density. Adaptation of conventional filtering approaches of ALS point clouds is required in order to derive correct, high resolution DTMs that preserve rock topography, but are free from artefacts caused by the insufficient removal of vegetation. In our study, we proposed and tested three methods that differ either in their suitability for a particular type of relief (rock walls with extensive upper plateaus vs. separated, rather narrow, rock pillars) or in their requirements for additional input data (none vs. existing DTMs).

Spatially conditioned filtering in an iterative, two-cycle process discriminates between the steep slopes of the rock walls and the rest of the landscape where conventional filtering methods are successful. The vegetation on the steep slopes is subsequently removed using modified filtering parameters. On the one hand, the tests showed certain drawbacks in successfully preserving the edges of the rocks at the expense of eliminating the vegetation. Therefore, the delineation of the rocky zones needs to be further elaborated. On the other hand, however, the method is fully automated, and the results proved that it may provide more reliable results than filtering with only one set of parameters.

The object-based method is more suitable for areas with dominating rock pillars and similar medium-sized features. After segmentation, the

trees and rocks are discriminated between each other based on the distribution of points inside the objects in three horizontal sections. Consequently, objects representing trees are filtered, whereas rock formations are considered terrain. The performed tests showed that the non-ground points were quite reliably filtered out (the user's accuracy of non-ground points was 78 %) but at the cost of a loss of ground points (the producer's accuracy of ground points was 81 %). The proposed method overcomes other types of filtering (overall accuracy of 85 % in comparison to 78 % for the method that included manual post-processing) and is quite successful in comparison to the ground truth but certain limits should be noted. The success of the individual steps depends on the initial generation of the point cloud surface. If the objects are merged during this step due to small distances between them, then the algorithm is not able to recognise them. The same issue occurs with the post-processing of the over segmentation. More training data may significantly improve the classification, but manual filtering is a very time-consuming and expert task.

Existing DTMs, though of lower density and/or quality, may be advantageous for deriving a new generation of DTMs. A relatively simple method based on setting a threshold of evaluated points to an approximate surface outperformed the manually corrected DTM of a lower density of 30 % of all points measured by GNSS. Moreover, at the edges of rock platforms, its accuracy was comparable to a manually corrected DTM (RMSE of 0.5 m), while the spatially conditioned filtering with manually created zones and two sets of parameters produced poor results (RMSE of 5 m, the filtered NP data of the GeNeSiS project). Considering the increasing frequency of data collection and point cloud density on both local and national levels, methods utilising existing filtered datasets have great potential in terms of updating and improving existing DTMs, and considerable savings on resources.

ALS may help unveil the unique and usually complicated topography of wooded sandstone landscapes in an unprecedented level of detail. However, the cost of this is more complicated processing of data in comparison to common terrain. The proposed methods showed the potential of replacing tedious manual filtering with automated procedures, although their choice and parameters need to be adjusted to local conditions in order to obtain a DTM of the highest possible quality.

Declaration of competing interest

The authors declare that they have no known competing financial interests or personal relationships that could have appeared to influence the work reported in this paper.

Data availability

The authors do not have permission to share data.

Acknowledgments

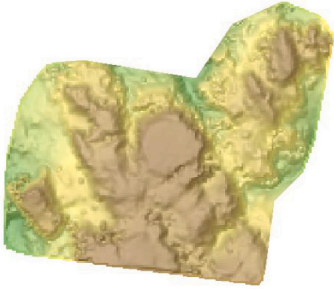
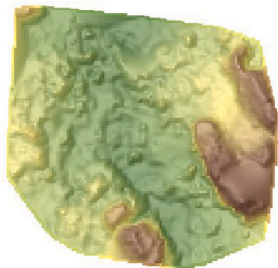
We would like to thank the Czech Land Survey Office and the Technische Universität Dresden for providing the data necessary for testing and evaluating the proposed methods. Our thanks also go to the Administration of the Bohemian Switzerland National Park and the Broumovsko Protected Landscape Area for allowing us to conduct field research in inaccessible areas of the protected regions. The first author is also grateful for the support provided by Charles University, project GA UK No. 132119.

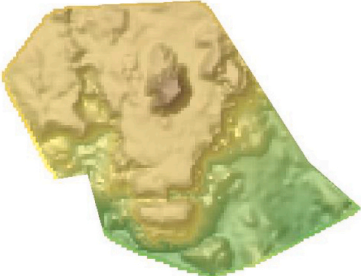
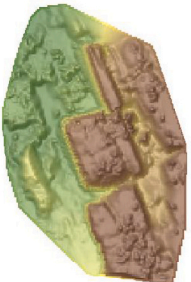
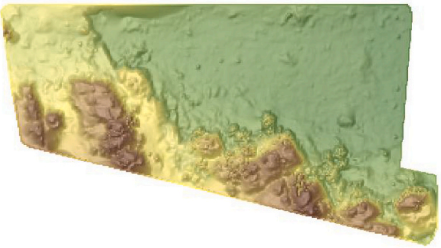
Appendix A

The Bohemian Switzerland National Park

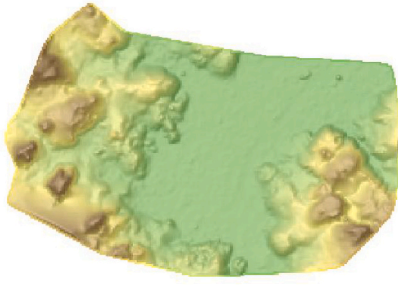
Location	Area	Coordinates of centroid
<p><i>NP A – Kamenice canyon</i></p> <p>A rather flat locality with a significantly incised valley of the Kamenice River and its inflows in the north. This canyon is flanked on both sides by rock walls, locally in a considerably advanced stage of erosion. Due to the high humidity in the vicinity of the streams, the vegetation here is luxuriant, so that the rock walls are covered with mosses and ferns, with occasional smaller trees growing out of them. There are also two small quays in the area on the Kamenice River, from which small excursion boats leave to cruise the gorges.</p>	2 x 2 sq. km	50°51'54"N, 14°16'25"E
<p><i>NP B – the Pravčická brána Arch (wide)</i></p> <p>A large area in the vicinity of the Pravčická brána Arch, including rock outcrops from several sandstone layers. Among the distinctive landforms are also canyons and dry valleys separating individual rock walls. The last layer of rocks is topped by a relatively flat vegetated plateau, which is broken in places by fissures, especially in the NE-SW direction.</p>	2 x 2 sq. km	50°52'59"N, 14°16'34"E
<p><i>NP C – the Pravčická brána Arch (small)</i></p> <p>Closer area around the Pravčická brána Arch, including parts of the lower levels of rock walls and one of the most eroded parts of the highest level of rock walls. In the northwest, there is a canyon approximately one hundred metres deep. Man-made objects can be found in the open tourist area, such as a restaurant, a small bridge, paved paths, and a terrace right under the arch, steps, and handrails along the path to viewpoints on the platform of the rock formation adjacent to the Pravčická brána Arch. The overall height difference reaches 180 m, with the highest point being around 505 m.</p>	400 x 400 sq. m	50°53'5"N, 14°16'51"E

The Adršpach-Teplice Rocks

Location name	Area [a]	Coordinates of centroid
<i>The Baronova vyhlídka Viewpoint</i>	39.9	50°36'33"N, 16°06'47"E
The jagged edge of the Milenecká Mountain borders a flat lookout on a rock plateau. There are several roughly separated rock pillars around the edge, with deep clefts between them. Pine trees growing directly from the rock outcrops are frequent.		
<i>Labyrinth – The Divoká rokle Ravine</i>	24.6	50°35'20"N, 16°08'22"E
As the name suggests, it is a difficult terrain full of rock formations lining deep valleys and hidden under vegetation. The site is located at the junction of the Divoká rokle Ravine and the valley of the Skalní potok Stream. A solitary rock pillar rises from the floor of the valley (not on the visualisation, as it has been filtered out) with a significant overhang and a tree on top, and there are two rock formations on the sides of the valley with a height of over 30 metres.		
<i>Milenci</i>	29.9	50°36'38"N, 16°06'49"E
Milenci are some of the most famous and highest rock pillars in the Adršpach Rocks. Their height is usually stated to be around 100 metres, but only 80 metres were measured from the detailed scanning data. There is another prominent rock tower in the locality called Uhlířská. Otherwise, it is a rather flat area, the bottom of which is overgrown, but both rock pillars have sparse vegetation on them.		
<i>The Skalní ostrov Plateau – middle part</i>	14.5	50°35'21"N, 16°07'20"E
An area roughly in the centre of the Skalní ostrov Plateau. It is characterised by difficult-to-access, very rugged, and overgrown terrain on the summit plateau with deep narrow crevices that tend to be overgrown with juniper and covered in foliage. Therefore, the laser beams have little chance of picking up information from the bottom or walls of the crevices. On the plateau itself there are still a few relics of the higher sandstone layer.		

<i>The Skalní ostrov Plateau - north</i>	49.7	50°35'31"N, 16°07'31"E
<p>The most disturbed area of the Skalní ostrov Plateau, which cannot be accessed without climbing equipment. The rock massif is so eroded that the rock pillars are relatively well separated from each other, and their tops are rounded, so there is no vegetation growing on them. However, from below they are lined with relatively tall trees.</p>		
<i>The Skalní ostrov Plateau - south</i>	18.9	50°35'15"N, 16°07'19"E
<p>It is a relatively compact and accessible part of the Skalní ostrov Plateau, separated from the adjacent valley by a rock wall about 35 metres high. On top of the relatively flat plateau is a relict rock pillar of higher strata of sandstone. The area is only partly forested, and the edge of the plateau is not covered with vegetation.</p>		
<i>The Martinské stěny Walls</i>	33.9	50°35'16"N, 16°07'32"E
<p>The site is on the edge of the opposite rock massif to the Skalní ostrov Plateau. From this side, it is flanked by a rock wall about 55 metres high with a segmented edge into individual rock pillars of different heights. Some of the rock pillars have a distinctly elongated shape in the NNW-SSE direction, which corresponds to the main direction of the massif's cleavage. Deep chasms have formed between the rock pillars. Fallen boulders have become overgrown with smaller trees, making it difficult to determine the bottom of these chasms.</p>		
<i>Wall near Starosta</i>	94.9	50°36'48"N, 16°6'39"E
<p>It is a relatively flat site overgrown with mature trees and lined with a rock wall about 50 metres high. The valley is cut by a wall about 10 metres high, beyond which is a hanging valley with a broken bottom and dense vegetation.</p>		

. (continued).

<i>The Vlčí rokle Gorge - The Černý příkop Ravine</i>	37.0	50°36'8"N, 16°07'9"E
A very narrow part of the Vlčí rokle Gorge, which is characterised by a specific microclimate. High humidity here allows the growth of dense low vegetation, which is complemented by mature trees.		
<i>The Vlčí rokle Gorge - Rašeliniště</i>	62.6	50°36'15"N, 16°07'4"E
This valley, which is up to 35 metres wide, is flat, waterlogged, and covered with grass. High rock towers rise on both sides of the valley but are often completely hidden under very mature trees.		
<i>The Vlčí vodopád Waterfall</i>	10.8	50°35'52"N, 16°07'32"E
The site is formed by a vertical rock wall, from the eroded part of which a waterfall flows after rains and snowmelt. There is a large amount of rubble under the waterfall. The surrounding walls are up to 35 metres high.		

. (continued).

References

- Alho, P., Vaaja, M., Kukko, A., Kasvi, E., Kurkela, M., Hyyppä, J., Hyyppä, H., Kaartinen, H., 2011. Mobile laser scanning in fluvial geomorphology: mapping and change detection of point bars. *Z. Geomorphol.* 55, 31–50. <https://doi.org/10.1127/0372-8854/2011/0055S2-0044>.
- Axelsson, P., 2000. DEM generation from laser scanner data using adaptive TIN models. *Int. Arch. Photogramm. Remote Sens.* 23, 110–117.
- Besl, P.J., McKay, N.D., 1992. A method for registration of 3-D shapes. *IEEE Trans. Pattern Anal. Mach. Intell.* 14, 239–256. <https://doi.org/10.1109/34.121791>.
- Beucher, S., Lantuéjoul, C., 1979. Use of watersheds in contour detection. In: *Proceedings of the International Workshop on Image Processing. CCETT*.
- Bollmann, E., Sailer, R., Briese, C., Stotter, J., Fritzmann, P., 2011. Potential of airborne laser scanning for geomorphologic feature and process detection and quantifications in high alpine mountains. *Z. Geomorphol.* 55, 83–104. <https://doi.org/10.1127/0372-8854/2011/0055S2-0047>.
- Briese, C., 2010. Extraction of digital terrain models. In: *Vosselman, G., Maas, H.-G. (Eds.), Airborne and Terrestrial Laser Scanning*. CRC Press, pp. 135–167.
- Castagnetti, C., Bertacchini, E., Corsini, A., Rivola, R., 2014. A reliable methodology for monitoring unstable slopes: the multi-platform and multi-sensor approach. In: *Michel, U. (Ed.), Earth Resources and Environmental Remote Sensing/GIS Applications V. SPIE*, pp. 87–96. <https://doi.org/10.1117/12.2067407>.
- Cílek, V., 2010. Saxon-Bohemian Switzerland: sandstone rock cities and fascination in a romantic landscape. In: *Migoň, P. (Ed.), Geomorphological Landscapes of the World*. Springer, Dordrecht, pp. 201–209.
- CloudCompare, 2021. CloudCompare [WWW document]. URL: <https://www.cloudcompare.org/main.html>. (Accessed 5 November 2021).
- Csaplovics, E., 2007. Digital terrain models of the sandstone landscapes in the Sächsische Schweiz (Saxon Switzerland) National Park and their value for conservation and ecological monitoring (Germany). In: *Härtel, H., Cílek, V., Herben, T., Williams, R., Jackson, A. (Eds.), Sandstone Landscapes*, pp. 61–65.
- Csaplovics, E., Naumann, K., Wagenknecht, S., 2003. Beiträge zur Extraktion von Felskanten aus Airborne Laser Scanner Daten am Beispiel der Elbsandsteinformationen im Nationalpark Sächsische Schweiz. *Photogramm. Fernerkundung. Geoinf.* 7, 106–115.
- Doneus, M., Briese, C., 2006. Digital terrain modelling for archaeological interpretation within forested areas using full-waveform laserscanning. In: *The 7th International Symposium on Virtual Reality, Archaeology and Cultural Heritage*, pp. 155–162. <https://doi.org/10.2312/VAST/VAST06/155-162>.
- Dušánek, P., 2014. *Nové výškopisné mapování České republiky*. GIS Ostrava, Ostrava.
- Duszynski, F., Janczewicz, K., Migoň, P., 2018. Evidence for subsurface origin of boulder caves, roofed slots and boulder-filled canyons (Broumov highland, Czechia). *Int. J. Speleol.* 47, 343–359. <https://doi.org/10.5038/1827-806X.47.3.2209>.
- Fiala, R., 2011. *Robustní postupy hodnocení kvality digitálních modelů reliéfu*. Faculty of Applied Sciences, University of West Bohemia.
- Gašior, M., 2006. *Laserové skenování pro tvorbu 3D modelu vybrané části*. Faculty of Environment, Jan Evangelista Purkyně University in Ústí nad Labem.
- Härtel, H., Cílek, V., Herben, T., Williams, R., Jackson, A. (Eds.), 2007. *Sandstone Landscapes*. Academia, Praha.
- Hayakawa, Y.S., Oguchi, T., 2016. Applications of terrestrial laser scanning in geomorphology. *J. Geogr. Zasshi* 125, 299–324. <https://doi.org/10.5026/jgeography.125.299>.
- He, Y., Liang, B., Yang, J., Li, S., He, J., 2017. An iterative closest points algorithm for registration of 3D laser scanner point clouds with geometric features. *Sensors (Switzerland)* 17, 1862. <https://doi.org/10.3390/s17081862>.
- Isenburg, M., 2020. *LAStools - Efficient LiDAR Processing Software*.

- Janczewicz, K., Migoń, P., Kasprzak, M., 2019. Connectivity patterns in contrasting types of tableland sandstone relief revealed by Topographic Wetness Index. *Sci. Total Environ.* 656, 1046–1062. <https://doi.org/10.1016/J.SCITOTENV.2018.11.467>.
- Janczewicz, K., Migoń, P., Kotwicka, W., Różycka, M., 2020. High-resolution geomorphometry -towards better understanding the genesis and contemporary processes in erosional sandstone landscapes. In: Alvioni, M., Marchesini, L., Melelli, L., Guth, P. (Eds.), *Proceedings of the Geomorphometry 2020 Conference*, pp. 107–110.
- Janczewicz, K., Poręba, W., 2022. Point cloud does matter. Selected issues of using airborne LiDAR elevation data in geomorphometric studies of rugged sandstone terrain under forest – case study from Central Europe. *Geomorphology*, 108316. <https://doi.org/10.1016/J.GEOMORPH.2022.108316>.
- Kraus, K., Pfeifer, N., 1998. Determination of terrain models in wooded areas with airborne laser scanner data. *ISPRS J. Photogramm. Remote Sens.* 53, 193–203. [https://doi.org/10.1016/S0924-2716\(98\)00009-4](https://doi.org/10.1016/S0924-2716(98)00009-4).
- Mandlbürger, G., Briese, C., Pfeifer, N., 2007. Progress in LiDAR sensor technology - chance and challenge for DTM generation and data administration. In: *Proceedings of the 51st Photogrammetric Week*. Stuttgart, Germany, pp. 159–169.
- Meng, X., Currit, N., Zhao, K., 2010. Ground filtering algorithms for airborne LiDAR data: a review of critical issues. *Remote Sens.* 2, 833–860. <https://doi.org/10.3390/RS2030833>, 2010, Vol. 2, Pages 833–860.
- Migoń, P., Duszyński, F., Goudie, A., 2017. Rock cities and ruiniform relief: forms – processes – terminology. *Earth-Sci. Rev.* 171, 78–104. <https://doi.org/10.1016/j.earscirev.2017.05.012>.
- Migoń, P., Duszyński, F., Janczewicz, K., Kotwicka, W., 2020. Late evolutionary stages of residual hills in tablelands (Elbsandsteingebirge, Germany). *Geomorphology* 367. <https://doi.org/10.1016/J.GEOMORPH.2020.107308>.
- Migoń, P., Kasprzak, M., 2016. Pathways of geomorphic evolution of sandstone escarpments in the Góry Stołowe tableland (SW Poland) - insights from LiDAR-based high-resolution DEM. *Geomorphology* 260, 51–63. <https://doi.org/10.1016/J.GEOMORPH.2015.08.022>.
- Mikuláš, R., Adamovič, J., Hájek, A., Spíšek, J., 2007. Adršpaško-teplické skály Cliffs and Ostaš Hill (Czech Republic). In: Härtel, H., Cílek, V., Herben, T., Williams, R., Jackson, A. (Eds.), *Sandstone Landscapes*. Academia, Praha, pp. 332–335.
- Mücke, W., Hollaus, M., Briese, C., Pfeifer, N., 2008. Analysis of Full-waveform Airborne Laser Scanning Data for the Improvement of DTM Generation. *Vienna University of Technology*.
- Paleček, V., Kubíček, P., 2018. Assessment of accuracy in the identification of rock formations from aerial and terrestrial laser-scanning data. *ISPRS Int. J. Geo Inf.* 7, 142. <https://doi.org/10.3390/IJGI7040142>, 2018, Vol. 7, Page 142.
- Qin, R., Tian, J., Reinartz, P., 2016. 3D change detection – approaches and applications. *ISPRS J. Photogramm. Remote Sens.* 122, 41–56. <https://doi.org/10.1016/J.ISPRSJPRS.2016.09.013>.
- RIEGL, 2021. RIEGL [WWW document]. URL. <http://riegl.com/>. (Accessed 5 November 2021).
- Shan, J., Toth, C.K., 2018. *Topographic Laser Ranging and Scanning: Principles and Processing*, 2nd ed. CRC Press. <https://doi.org/10.1201/9781420051438>.
- Sithole, G., 2005. *Segmentation and Classification of Airborne Laser Scanner Data*. Netherlands Geodetic Commission, Delft.
- Sithole, G., Vosselman, G., 2004. Experimental comparison of filter algorithms for bare-Earth extraction from airborne laser scanning point clouds. *ISPRS J. Photogramm. Remote Sens.* 59, 85–101. <https://doi.org/10.1016/j.isprsjprs.2004.05.004>.
- Štroner, M., Urban, R., Lidmila, M., Kolář, V., Křemen, T., 2021. Vegetation filtering of a steep rugged terrain: the performance of standard algorithms and a newly proposed workflow on an example of a railway ledge. *Remote Sens.* 13, 3050. <https://doi.org/10.3390/RS13153050>.
- Székely, B., Zámolyi, A., Draganits, E., Briese, C., 2009. Geomorphic expression of neotectonic activity in a low relief area in an Airborne Laser Scanning DTM: a case study of the Little Hungarian Plain (Pannonian Basin). *Tectonophysics* 474, 353–366. <https://doi.org/10.1016/J.TECTO.2008.11.024>.
- TerraSolid, 2021. TerraScan [WWW document]. URL. <https://terrasolid.com/products/terrascan/>. (Accessed 5 November 2021).
- TopoSys, 2021. TopoSys Lidar solutions [WWW document]. URL. <http://www.imagemaps.com/toposys.htm>. (Accessed 5 November 2021).
- Trimble, 2021a. SCOP++ [WWW document]. URL. <https://www.trimble.com/inpho/>. (Accessed 5 November 2021).
- Trimble, 2021b. DTMaster [WWW document]. URL. <https://www.trimble.com/inpho/>. (Accessed 5 November 2021).
- Trommler, M., 2007. *Geodata for the Saxon – Bohemian Switzerland*. Dresden, Germany.
- Vařilová, Z., 2016. Elbe sandstones. In: Pánek, T., Hradecký, J. (Eds.), *Landscapes and Landforms of the Czech Republic*. Springer, Switzerland, pp. 123–137. <https://doi.org/10.1007/978-3-319-27537-6>.
- Vařilová, Z., Příkrýl, R., Zvelebil, J., 2015. Factors and processes in deterioration of a sandstone rock form (Pravčická brána Arch, Bohemian Switzerland NP, Czech Republic). *Z. Geomorphol.* 59, 81–101. https://doi.org/10.1127/ZFG_SUPPL/2015/S-00175.
- Vetter, M., Hofle, B., Mandlbürger, G., Rutzinger, M., 2011. Estimating changes of riverine landscapes and riverbeds by using airborne LiDAR data and river cross-sections. *Z. Geomorphol.* 55, 51–65. <https://doi.org/10.1127/0372-8854/2011/0055S2-0045>.
- Vítek, J., 2016. Adršpaško-Teplička Rocks and Broumov Cliffs - large sandstone rock cities in the Central Europe. In: Pánek, T., Hradecký, J. (Eds.), *Landscapes and Landforms of the Czech Republic*. Springer, Switzerland, pp. 209–220.
- Vosselman, G., 2000. Slope based filtering of laser altimetry data. *Int. Arch. Photogramm. Remote Sens.* XXXIII 935–942.
- Vosselman, G., Maas, H.-G., 2010. *Airborne and Terrestrial Laser Scanning*. CRC Press.
- Wagner, W., Ullrich, A., Ducic, V., Melzer, T., Studnicka, N., 2006. Gaussian decomposition and calibration of a novel small-footprint full-waveform digitising airborne laser scanner. *ISPRS J. Photogramm. Remote Sens.* 60, 100–112. <https://doi.org/10.1016/j.isprsjprs.2005.12.001>.
- Wagner, W., Ullrich, A., Melzer, T., Briese, C., Kraus, K., 2004. From single-pulse to full-waveform scanners: potential and practical challenges. *Int. Arch. Photogramm. Remote Sens. Spat. Inf. Sci.* 35, 201–206.
- Williams, J., Bennamoun, M., 2001. Simultaneous registration of multiple corresponding point sets. *Comput. Vis. Image Underst.* 81, 117–142. <https://doi.org/10.1006/cviu.2000.0884>.
- Xie, Y., Tian, J., Zhu, X.X., 2020. Linking points with labels in 3D: a review of point cloud semantic segmentation. *IEEE Geosci. Remote Sens. Mag.* 8, 38–59. <https://doi.org/10.1109/MGRS.2019.2937630>.
- Zhang, K., Whitman, D., 2005. Comparison of three algorithms for filtering airborne lidar data. *Photogramm. Eng. Remote Sensing* 71, 313–324. <https://doi.org/10.14358/PERS.71.3.313>.
- Zhao, X., Guo, Q., Su, Y., Xue, B., 2016. Improved progressive TIN densification filtering algorithm for airborne LiDAR data in forested areas. *ISPRS J. Photogramm. Remote Sens.* 117, 79–91. <https://doi.org/10.1016/J.ISPRSJPRS.2016.03.016>.
- Zhao, X., Su, Y., Li, W.K., Hu, T., Liu, J., Guo, Q., 2018. A comparison of LiDAR filtering algorithms in vegetated mountain areas. *Can. J. Remote. Sens.* 44, 287–298. <https://doi.org/10.1080/07038992.2018.1481738>.